# Spin Readout and Initialization in a Semiconductor Quantum Dot

Mark Friesen,* Charles Tahan, Robert Joynt, and M. A. Eriksson
*Department of Physics, University of Wisconsin, Madison, Wisconsin 53706, USA*
(Received 17 April 2003; published 20 January 2004)

Electron spin qubits in semiconductors are attractive from the viewpoint of long coherence times. However, single spin measurement is challenging. Several promising schemes incorporate ancillary tunnel couplings that may provide unwanted channels for decoherence. Here, we propose a novel spin-charge transduction scheme, converting spin information to orbital information within a single quantum dot by microwave excitation. The same quantum dot can be used for rapid initialization, gating, and readout. We present detailed modeling of such a device in silicon to confirm its feasibility.

DOI: 10.1103/PhysRevLett.92.037901 PACS numbers: 03.67.Pp, 03.67.Lx, 85.35.Be, 73.21.La

Quantum dot qubits lie at the point of intersection between quantum computing and few-electron spintronics. The long coherence times and novel quantum mechanical properties of electron spins, the attraction of scalability, and the shared technology base with the digital electronics industry fuel a large research effort to develop these systems. Several proposals have been put forward for spin qubits in semiconductors [1–5]. In particular, exchange coupled gates in semiconductor dots appear to be workable [5], and several components of qubit technology have been demonstrated recently [6]. However, the combined challenge of preparing, storing, and measuring spins is formidable.

Measurements of spin qubits pose a special challenge. On the one hand, qubits should be well isolated from their environment to avoid decoherence. On the other hand, it is necessary to individually couple the qubits to an external measurement device. Qubit initialization involves an additional dissipative coupling to the environment. For quantum computing, we must initiate such couplings selectively, and with sufficient strength to perform the operations quickly. Indeed, scalable quantum computing relies on fault-tolerant quantum error correction algorithms, involving frequent, parallel measurements, and a steady supply of initialized qubits [7]. Fortunately, rapid and sensitive quantum measurement techniques involving radio frequency single electron transistors (rf-SETs) have been developed [8]. rf-SETs have been used to detect the tunneling of individual electrons in semiconductor devices [9].

We have previously designed a quantum dot architecture specifically for the purpose of manipulating electron spins for fast and accurate two-qubit operations that serve as universal gates for quantum computations [5]. Recent experimental results have shown that decoherence does not pose a fundamental problem for such gate operations [10]. Using special qubit geometries [11], it should be possible to perform reliable gate operations in silicon quantum dots at rates between about 1 MHz and 1 GHz [12]. The question is now whether similar speeds and reliable operation can be achieved for measurement and initialization operations. In this Letter, we show how to extend our architecture to enable the readout and initialization of the state of a single spin. The general scheme does not assume a specific material system. However, in this Letter we focus upon silicon-based devices because of their desirable coherence properties.

Our method relies on the idea of converting spin information to charge information discussed by Loss and DiVincenzo [1], and using single electron transistors to read out the resulting spin state as proposed by Kane *et al.* [2], who posit spin-dependent charge motion onto impurities in Si. Martin *et al.* [13] have proposed a scheme for single spin readout that also converts spin information into charge information in an electron trap near a conducting channel. The resistance of the channel depends on the occupation of the trap, which in turn can be made to depend on the spin. Our proposed device has the additional feature in that it enables both readout *and* rapid initialization of the spin state. Rapid initialization (as opposed to initialization by thermalization) is just as essential as readout, and just as difficult to carry out. Our design is simple in that it obviates the need for spin-polarized leads or ancillary qubits. We go beyond conceptual design—the full three-dimensional system is simulated self-consistently and the operating parameters are thereby optimized. This enables us to demonstrate quantitatively that the device is in a working regime.

The basic Si-SiGe heterostructure is described in Ref. [5]. The main point for present purposes is that the active layer is pure strained Si, which minimizes decoherence from spin-phonon coupling [14]. The qubits are gated quantum dots which hold one electron, and the gate geometry is the key to our scheme. Specifically, the electrons are confined in asymmetric lateral wells, such that orbital excitation results in lateral center-of-charge movement. Figure 1 shows the first two orbital states of an electron confined to an asymmetric box, with center-of-charge positions varying by a distance $\Delta y$. If an external radiation source of frequency $E_{12}/h$ drives the system between the ground and first excited states, $n = 1$ and $n = 2$, the center-of-charge of the electron will oscillate in

  

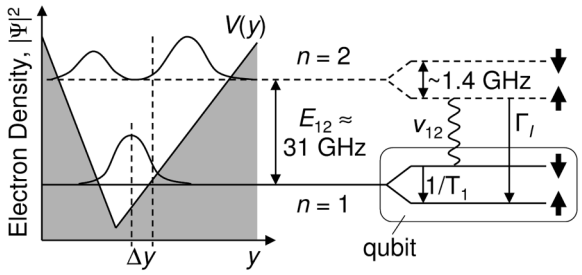


FIG. 1. Schematic example of a one-dimensional, asymmetric confining potential. Quantum dot energy states and transition rates for readout and initialization are shown.

time at the Rabi frequency $\nu_R$. This motion can be detected by a sensitive electrometer, such as a single electron transistor or a quantum point contact. With the system placed in a magnetic field, charge motion can be generated in a *spin-dependent* fashion. We define the logical 0 and 1 of the qubit as the spin-up and spin-down states of the electron in its orbital ground state and use the orbital excited state only during initialization and readout. The system is now driven at the readout frequency $\nu_{12}(B) = E_{12}/h - g\mu_B B/h$. This causes charge motion only if the qubit was in the down state at the time of measurement. Although this transition is forbidden at the electric dipole level because of the spin-flip, spin-orbit coupling allows for a nonzero transition rate, as described below.

Crucially, this architecture also allows for rapid initialization of the qubit. Consider exposing a random ensemble of qubits to radiation of frequency $\nu_{12}$. An electron in the $(1,\downarrow)$ state will be excited to the level $(2,\uparrow)$ and experience a relatively fast relaxation to the ground state $(1,\uparrow)$, compared to a spin-flip relaxation to the level $(1,\downarrow)$. The net result is to rapidly polarize and thereby initialize the qubits. By varying the gate voltages (and thus $\nu_{12}$) on individual dots we ensure that only desired qubits are brought into resonance. Clearly, understanding the competition between the three time scales, $1/\nu_R$, $1/\Gamma_I$, and $T_1$, as a function of material parameters and gate potentials is the key to utilizing this device for readout and initialization. Note that $T_1$ represents a thermal initialization time from $(1,\downarrow)$ to $(1,\uparrow)$. Since $T_1$ is a decoherence time, we require $1/\nu_R \ll T_1$. The Rabi oscillation frequency $\nu_R$ depends on the incident intensity and is therefore controllable, within limits. Robust measurement requires that many Rabi oscillations occur before orbital decay: $1/\nu_R \lesssim 1/\Gamma_I$.

In order to understand the competition of time scales, we introduce an rms interaction energy, time averaged (as indicated by $\{\}$) over an optical cycle, which expresses the strength of the interaction in the electric dipole approximation. This defines the Rabi oscillation frequency [15]: $|h\nu_R|^2 = \{|V^{E1}|^2\}$. Here, $V^{E1} = (-e\hbar E_0/m^* E_{12})\hat{\boldsymbol{\epsilon}}\cdot\mathbf{p}$ is the dipole term in the Hamiltonian, $|E_0|^2$ is twice the mean value of $|\mathbf{E}(t)|^2$ averaged in time, and $\hat{\boldsymbol{\epsilon}}$ is the polarization unit vector. The electric field $E_0$ inside the semiconductor with dielectric constant $\varepsilon = \varepsilon_r\varepsilon_0$ is related to the intensity of the external radiation $I$ by $E_0 = \sqrt{2I/c\varepsilon_0\sqrt{\varepsilon_r}}$.

The dipole Hamiltonian does not flip the spin directly, but spin-orbit coupling causes each qubit state to be an additive mixture of up and down spin. In the 2D limit, the spin-orbit (so) Hamiltonian is dominated by the bulk [Dresselhaus (D)] and structural [Rashba (R)] inversion asymmetry terms, $H_{so} = H_D + H_R$, where $H_D = \beta(p_y\sigma_y - p_x\sigma_x)$ and $H_R = \alpha(p_x\sigma_y - p_y\sigma_x)$. Including $H_{so}$ perturbatively gives a nonzero dipole matrix element, and for light polarized in the $y$ direction, the readout frequency is given by

$$|\nu_R| \simeq \frac{eE_0}{2\pi h\nu_{12}(B)}\sqrt{\alpha^2+\beta^2}\,|\langle 2|y\partial_y|1\rangle|. \qquad (1)$$

Note that the applied radiation need not be circularly polarized for this readout scheme. The Dresselhaus and Rashba parameters $\alpha$ and $\beta$ depend on intrinsic material properties, device design, and external electric field. For GaAs, both theoretical and experimental values vary widely [16]: $\alpha$ = 1–1000 m/s and $\beta$ = 1000–3000 m/s. In a centrosymmetric crystal such as silicon which has no bulk inversion asymmetry, $\beta = 0$. The one known data point for a SiGe two-dimensional electron gas gives $\alpha \simeq$ 8 m/s [17], which we use in our estimates below.

The relaxation of our quantum dot to its ground state enables spin polarization, but limits or even inhibits readout if it occurs too quickly. This problem has been addressed by Khaetskii and Nazarov in GaAs quantum dots [18]. In silicon, where there is no piezoelectric interaction, we calculate the relaxation rate via the golden rule with the usual deformation potential electron-phonon Hamiltonian [19]. At sufficiently low temperatures ($T < 1$ K), optical polar phonons and multiphonon processes do not contribute. By considering only longitudinal phonons, with dispersion $\omega = v_l q$, and using the long-wavelength approximation $e^{i\mathbf{k}\cdot\mathbf{r}} \simeq 1 + i\mathbf{k}\cdot\mathbf{r}$, we obtain the orbital decay rate due to electron-lattice coupling:

$$\Gamma_I = \frac{(E_{12})^5}{6\pi\hbar^6 v_l^7\rho}(\Xi_d + \Xi_u/3)^2\sum_i |\langle 1|x_i|2\rangle|^2, \qquad (2)$$

where $\rho$ is the mass density, and $\Xi_d$ and $\Xi_u$ are the deformation constants. In strained systems, transverse phonons can also be important, as we shall discuss in a future publication [20].

We perform a numerical analysis to obtain performance characteristics for the proposed measurement scheme. The numerical techniques used are an extension of those used in Refs. [5,11]. The gate potentials, the electronic orbitals, and their corresponding image potentials (arising predominantly from the metallic gates) are computed self-consistently by a combination of three-dimensional finite element and diagonalization

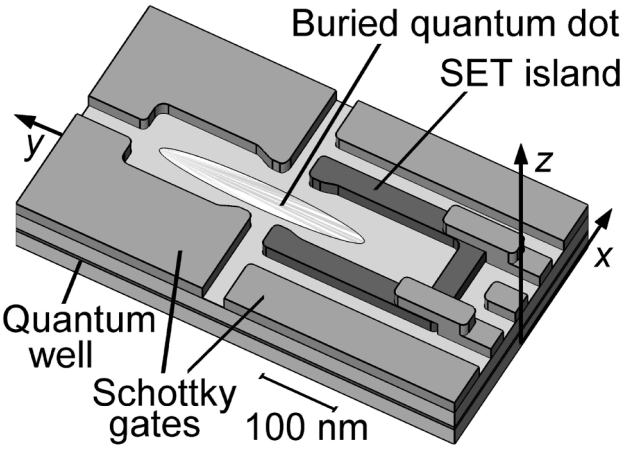


FIG. 2. The readout device studied in Figs. 3 and 4. Many similar devices were modeled in this work.

techniques. Specifically, we determine the readout oscillation frequency Eq. (1), the orbital decay rate Eq. (2), and the coupling sensitivity of the qubit electron to an integrated SET. We have modeled numerous devices and a full account will be published elsewhere [20]. One of the most promising is shown in Fig. 2. This is a 6 nm strained silicon quantum well sandwiched between layers of strain-relaxed silicon-germanium ($Si_{85}Ge_{15}$). The bottom barrier (30 nm) separates the quantum well from a grounded metallic back gate. The top barrier (30 nm) separates the quantum well from lithographically patterned Schottky top gates, whose voltages can be controlled independently. We consider negative gate potentials, which provide lateral confinement of the quantum dot through electrostatic repulsion. The main features of the quantum dot are that it is narrow, long, and slightly asymmetric. The *narrow* feature ensures that the excited orbitals are nondegenerate, so a microwave field with narrow linewidth will not induce unwanted transitions. The *long* feature ensures that the energy splitting $E_{12}$ (and thus $\Gamma_I$) will be small. The *asymmetry* ensures that excited orbitals will provide charge motion. Figure 3 shows the confinement potential for the device of Fig. 2; the asymmetry of the dot potential is apparent.

Our most interesting results are obtained in the regime where the gate and image potentials are comparable in size. The effective confinement potential, including images, is rather complicated due to the inhomogeneous gate arrangement. Indeed, it is a very poor approximation to neglect screening in this system. The computed wave functions for our dot are shown in Fig. 3.

We have also incorporated a SET into our proposed readout device, as shown in Fig. 2. The island of the SET is sheathed by a thin, 2-nm layer of silicon dioxide, and tunnel coupled to adjoining source and drain gates. A third, capacitively coupled gate is placed nearby to provide full control over both the charge and the potential of the island. When the device is operated in the Coulomb blockade regime, it becomes a sensitive electrometer [21].

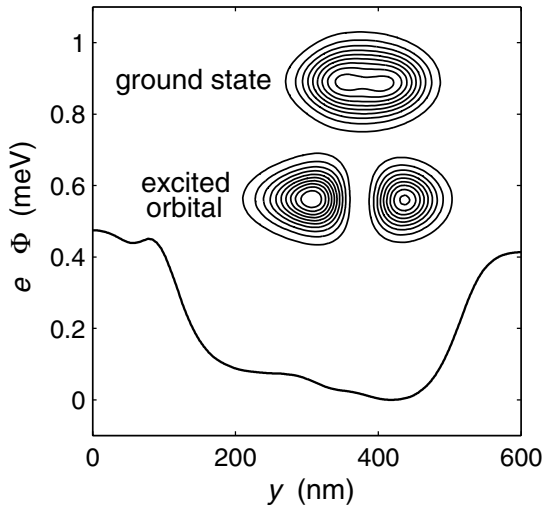


FIG. 3. Electrostatic confinement potential and qubit electron wave functions. The bare potential shown here is obtained in the quantum well along the device symmetry line, $x = 0$. The contour plots show the electron probability densities in the $x$-$y$ plane.

In the gate arrangement of Fig. 2, the SET plays two roles. First, voltage control of the island allows us to vary the size of the dot and thus the energy splitting $E_{12}$. Second, capacitive coupling to the quantum dot enables detection of its orbital state. The scheme works as follows. Since the dot orbitals are spatially distinct, they induce different amounts of charge on the SET island. Consequently, transport currents through the SET will reflect the orbital states of the dot. The device exhibits optimal sensitivity if biased at the half maximum of the conductance peak. The third SET gate has been introduced specifically to adjust this working point. As expected for our geometry, we find that the SET couples most strongly to the excited electronic orbital.

For the device shown in Fig. 2 we obtain an energy splitting of $E_{12} = 0.129$ meV $= 31.2$ GHz between the two lowest orbital states, and the dominant matrix elements $|\langle 1|y|2\rangle| = 48$ nm and $|\langle 2|y\partial_y|1\rangle| = 3.6$. From these results we obtain the readout oscillation frequency $\nu_R = 5.5 \times 10^5\sqrt{I}$ Hz (for microwave intensity $I$ in units of W/m$^2$), and the orbital decay rate for spontaneous phonon emission $\Gamma_I = 12.7$ MHz. The orbital decay rate for emission of a photon is very much less: $\Gamma_\gamma = e^2E_{12}^3|\langle 1|y|2\rangle|^2\sqrt{\varepsilon}/3\pi\hbar^4c^3\varepsilon_0^{3/2} = 6.5$ Hz, and therefore is not a limiting factor in this scheme. All results are obtained at an ambient temperature of $T = 100$ mK and a magnetic field of $H = 0.05$ T $= 1.40$ GHz. The dielectric constant of Si is $\varepsilon = 11.9\varepsilon_0$. Note that the natural widths of the states are small compared to their separation. The charge on the SET island was computed by integrating $\mathbf{n} \cdot \mathbf{D}$ over the surface. The excess or induced charge of the excited quantum dot orbital, relative to its ground state, was found to be $\Delta Q = 0.052e$. The corresponding center-of-charge motion in the dot is $\Delta y = 4.3$ nm. However, the

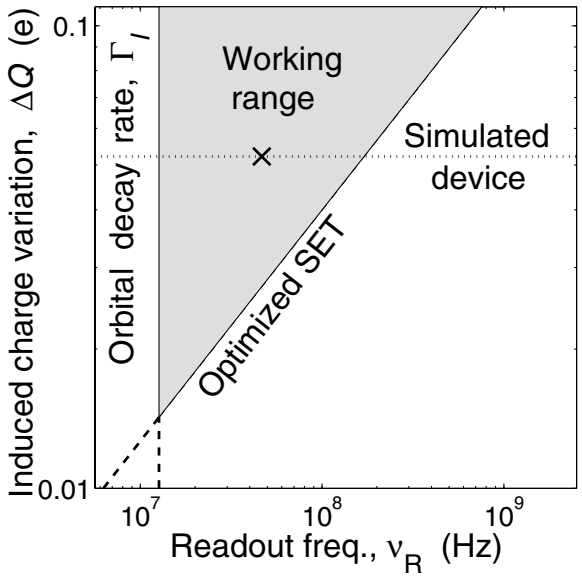


FIG. 4. Summary of operation parameters for the device shown in Fig. 2. The shaded region shows the operating range, with constraints set by the sensitivity of the SET and the spontaneous decay rate of the upper readout state. The dotted line shows the actual operating range of the device when the intensity of the incoming radiation is left variable. A likely working point of $\nu_R$, marked by $\times$, corresponds to an intensity $I = 7.2\ \mathrm{nW}/\mu\mathrm{m}^2$.

charge motion does not track closely with $\Delta Q$; the latter is determined primarily by the capacitive coupling between the dot and the SET. Finally, we find that by changing the bias voltage on the SET by 20% (thus reducing the dot size), the excitation resonance frequency $\nu_{12}$ changes by 8 GHz.

The prospects for initialization and readout in this scheme are partially summarized in Fig. 4. Theoretical considerations of shot noise [21,22] place an upper bound of about $4 \times 10^{-6} e/\sqrt{\mathrm{Hz}}$ on the detection sensitivity for charge induced on the island of an optimized rf-SET, as a function of the measurement bandwidth. Similarly, the decay rate of the excited electronic orbital places a lower bound on the readout oscillation frequency $\nu_R$. The latter is a function of microwave intensity. By directing 70 pW of microwave power onto a dot of size $\sim 0.1 \times 0.1\ \mu\mathrm{m}^2$, as consistent with low-temperature transport experiments, we would obtain the $\nu_R$ working point marked in Fig. 4, with $1/\nu_R \lesssim 1/\Gamma_I$. Sample heating outside the dot can be minimized by using integrated on-chip antennas to focus the power [23]. We must also satisfy the requirement $T_s \gg 1/\Gamma_I = 78.7$ ns where $T_s$ is the spin decoherence time. Theoretical estimates for $T_1$ in Si quantum dots exceed 1 ms [14]. Experiments on dots have yet to be performed, but spins of electrons in impurity donor states should have similar lifetimes. Recent work on electron spins in $^{28}$Si:P [10] would imply that $T_s > 60$ ms. Hence the crucial hierarchy of time scales $1/\nu_R \lesssim 1/\Gamma_I \ll T_s$ should be achievable.

In summary, we have proposed, simulated, and analyzed a scheme for measuring single electron spins in a quantum dot via spin-charge transduction. Adequate charge detection sensitivity is provided by an integrated rf-SET. The scheme also enables fast initialization.

We thank Alex Rimberg and the quantum computing group at the University of Wisconsin–Madison for many beneficial discussions. Our work was supported by the U.S. Army Research Office through ARDA and by the National Science Foundation through the QuBIC program, DMR-0079983, and DMR-0081039.

*Electronic address: friesen@cae.wisc.edu

[1] D. Loss and D. P. DiVincenzo, Phys. Rev. A **57**, 120 (1998).
[2] B. E. Kane, Nature (London) **393**, 133 (1998).
[3] R. Vrijen *et al.*, Phys. Rev. A**62**, 012306 (2000).
[4] J. Levy, Phys. Rev. A **64**, 052306 (2001).
[5] M. Friesen *et al.*, Phys. Rev. B **67**, 121301(R) (2003).
[6] J. M. Elzerman *et al.*, Phys. Rev. B **67**, 161308(R) (2003).
[7] P. W. Shor, in *Proceedings of the 35th Annual Symposium on Foundations of Computer Science*, edited by S. Goldwasser (IEEE Computer Society Press, Los Alamitos, CA, 1994), p. 124; A. M. Steane, Phys. Rev. A **68**, 042322 (2003).
[8] K. W. Lehnert *et al.*, Phys. Rev. Lett. **90**, 027002 (2003).
[9] W. Lu *et al.*, Nature (London) **423**, 422 (2003).
[10] A. M. Tyryshkin *et al.*, Phys. Rev. B **68**, 193207 (2003).
[11] M. Friesen, R. Joynt, and M. A. Eriksson, Appl. Phys. Lett. **81**, 4619 (2002).
[12] The results listed here reflect an update of Ref. [11]. We have taken into account the fault-tolerant error threshold of $\sim 10^{-2}$ for *amplitude* errors in the qubit state [E. Yablonovitch and D. Gottesman (unpublished)].
[13] I. Martin, D. Mozyrsky, and H. W. Jiang, Phys. Rev. Lett. **90**, 018301 (2003).
[14] C. Tahan, M. Friesen, and R. Joynt, Phys. Rev. B **66**, 035314 (2002).
[15] B. W. Shore, *The Theory of Coherent Atomic Excitation* (Wiley, New York, 1990).
[16] E. A. de Andrada e Silva, G. C. La Rocca, and F. Bassani, Phys. Rev. B **55**, 16 293 (1997).
[17] Z. Wilamowski, W. Jantsch, H. Malissa, and U. Rossler, Phys. Rev. B **66**, 195315 (2002).
[18] A. V. Khaetskii and Y. V. Nazarov, Phys. Rev. B **61**, 12 639 (2000)
[19] B. K. Ridley, *Quantum Processes in Semiconductors* (Oxford Press, New York, 1999), 4th ed.
[20] M. Friesen, C. Tahan, R. Joynt, and M. A. Eriksson (unpublished).
[21] M. H. Devoret and R. J. Schoelkopf, Nature (London) **406**, 1039 (2000).
[22] A. N. Korotkov and M. A. Paalanen, Appl. Phys. Lett. **74**, 4052 (1999).
[23] R. H. Blick *et al.*, Appl. Phys. Lett. **67**, 3924 (1995).